

Probing metal-mediated O₂ activation in chemical and biological systems

Valeriy V. Smirnov, David W. Brinkley, Michael P. Lanci, Kenneth D. Karlin, Justine P. Roth*

Department of Chemistry, The Johns Hopkins University, 3400 North Charles Street, Baltimore, MD 21218, United States

Available online 20 March 2006

Abstract

The use of oxygen (¹⁸O) isotope fractionation as a mechanistic probe of chemical and biological oxidation reactions, particularly those which involve metal–O₂ adducts, is currently being explored. Summarized here are reactions of enzymes and inorganic compounds for which competitive isotope effect measurements have been performed using natural abundance molecular oxygen and isotope ratio mass spectrometry. The derived ¹⁸O equilibrium isotope effects (EIEs) and kinetic isotope effects (KIEs) reflect the ground state and transition state structures, respectively, for reactions of ¹⁶O–¹⁶O and ¹⁸O–¹⁶O. Normal isotope effects (>1) characterize the binding of O₂ to transition metal centers. The magnitudes, which are primarily determined by the decrease in the O–O force constant accompanying formal electron transfer from the metal to O₂, suggest that metal superoxo complexes can be distinguished from metal peroxo complexes. Because ¹⁸O isotope effects can be measured during catalytic turnover, they complement existing approaches to elucidating the structures of activated oxygen intermediates based on low-temperature spectroscopy and crystallographic analysis of inorganic model compounds.

© 2006 Elsevier B.V. All rights reserved.

Keywords: Equilibrium isotope effects (EIEs); Kinetic isotope effects (KIEs); O₂ activation

1. Introduction

‘Bio-inspired’ approaches in catalysis have aimed to reproduce the strategies used by enzymes to carry out intrinsically difficult reactions, such as the activation of O₂ for the selective oxidation of hydrocarbon substrates [1]. Enzymes that accomplish this transformation include the oxygenases, which mediate the insertion of one or both atoms from O₂ into the substrate C–H [2,3], and the oxidases, which use O₂ simply as an electron sink [4]. Advances in the crystallographic and spectroscopic characterization of active sites have provided important information concerning the static structures of proteins [5,6]. However, the determination of enzyme mechanisms as well as the factors which control rates and selectivity has remained a challenge. New probes are needed to examine reactions under conditions relevant to catalysis where transient intermediates are often difficult to detect. We are, therefore, developing methods to relate oxygen (¹⁸O) isotope effects to activated oxygen intermediates characterized by vibrational spectroscopy as well as the nature of such intermediates in enzymes to those derived from synthetic inorganic compounds.

Lack of mechanistic understanding concerning O₂ reactivity in chemical and biological systems has limited the development

of new classes of oxidation catalysts that can function with the efficiency and selectivity of enzymes. In fact, an enormous effort has been directed towards the synthesis and characterization of inorganic compounds as enzyme models [7,8]. While very few of these compounds are functional catalysts, they have been used widely to illuminate the structures of enzyme active sites. Presented here is an overview of the ¹⁸O isotope effects that have been determined upon related reactions of metalloproteins and inorganic compounds as well as the interpretations of the results in the context of structure and mechanism. These studies illustrate how isotopic probes can provide new insights which would be very difficult to obtain using conventional spectroscopic techniques. Because the ¹⁸O isotope effects reflect the change in bonding along the reaction coordinate, they provide information which can be used to evaluate the nature of reaction barriers. It must be emphasized, however, that the isotope effect is only one piece of a complex puzzle. Its interpretation requires study of the reaction kinetics, the analysis of the vibrational frequencies and the application of the appropriate level of theory, which in some cases has not been established.

2. Overview of instrumentation and methodology

The measurement of competitive isotope effects is performed using an apparatus which consists of two adjoined high-vacuum manifolds (Fig. 1) [9]. One manifold is interfaced with a

* Corresponding author. Fax: +1 410 516 8420.
E-mail address: jproth@jhu.edu (J.P. Roth).

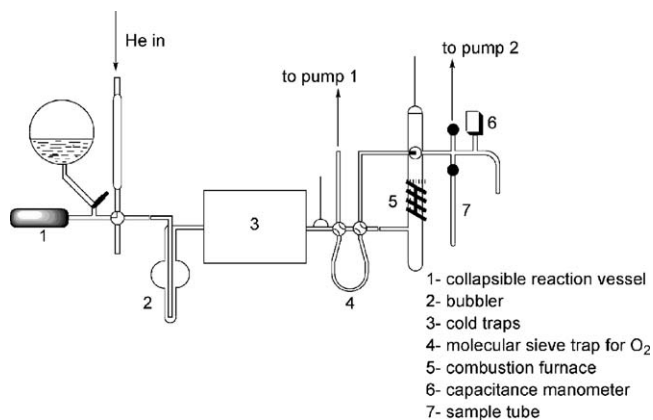


Fig. 1. Vacuum apparatus for the measurement of competitive ¹⁸O isotope effects.

reaction chamber from which constant volumes of O₂-containing solution are withdrawn prior and subsequent to the addition of an enzyme or inorganic compound. At varying percentages of conversion, the O₂ which has not reacted is isolated from the solution and purified by passage through a series of cold traps under vacuum. The O₂ collected in a liquid nitrogen-cooled trap containing 5 Å molecular sieves is subsequently released into a second manifold where it is quantitatively converted to CO₂. Combustion is achieved by re-circulating the O₂ through a graphite furnace at 900 °C and condensation of the CO₂ produced. The pressure of the CO₂ is determined using a capacitance manometer and related back to the amount of O₂ consumed in the reaction. The CO₂ samples are then transferred to evacuated tubes, flame-sealed and later analyzed by isotope ratio mass spectrometry.

A key feature of the method is that it is performed using natural abundance O₂. Thus, isotope effects are determined for the reactions of the abundant isotopologues: ¹⁶O–¹⁶O and ¹⁸O–¹⁶O present in the same solution, i.e. under conditions of intermolecular competition. Aside from the obvious advantage of not requiring isotope enrichment, the approach avoids error which could arise from dilution of ¹⁸O-enriched material by ambient air. Since the natural abundance of ¹⁸O is low (0.205 ± 0.014%) sample sizes are typically greater than 5 μmol. In principle, the O₂ could be analyzed directly, but since the CO₂ is easier to manipulate the combustion step is performed. Because combustion is carried out to 100% completion, the CO₂ has exactly the same oxygen isotope composition as the O₂ from which it is prepared.

Generally, experiments involve determining the change in the ¹⁸O/¹⁶O ratio due to a catalytic or stoichiometric reaction which consumes O₂. This quantity is determined using a fixed field isotope ratio mass spectrometer equipped with dual inlet for referencing against a standardized sample of CO₂ gas. The technique gives ¹⁸O/¹⁶O ratios relative to a standard, which are precise to approximately 0.1–0.2 parts per thousand (δ¹⁸O in per mille notation). Errors are compounded by manipulations of samples on the vacuum apparatus resulting in precisions that are approximately 10 times lower. Repeated measurements on

samples of O₂ from the air have indicated δ¹⁸O = 23.5 ± 1.5‰ versus standard mean ocean water (SMOW).

Two types of competitive ¹⁸O fractionation measurements have been performed, those that give equilibrium isotope effects (¹⁸O EIEs) and those that give kinetic isotope effects (¹⁸O KIEs) [10]. The ¹⁸O EIEs (abbreviated ¹⁸K) correspond to a ratio of equilibrium constants: $K(^{16}\text{O}-^{16}\text{O})/K(^{18}\text{O}-^{16}\text{O})$ and the ¹⁸O KIEs (abbreviated ¹⁸k) correspond to a ratio of second order rate constants: $k(^{16}\text{O}-^{16}\text{O})/k(^{18}\text{O}-^{16}\text{O})$. Both isotope effects are defined as a ratio of ratios (see below). Very small 2σ errors, averaging 5–10% of the isotope effect, are typically obtained from six or more independent measurements.

The approaches used to study EIEs and KIEs differ with respect to the experimental setup and methodology used. EIEs for species in equilibrium with O₂ are obtained using an open reaction vessel that allows rapid exchange between the atmosphere and solution. Experiments are performed by adding a sufficient amount of the reduced species to a solution such that the change in total O₂ concentration (i.e. O₂^{unbound} + O₂^{bound}) can be accurately determined. The isotope composition of the O₂ freely dissolved in the solution remains constant because of its rapid exchange with the atmosphere. Yet the O₂ bound to a transition-metal complex or metalloprotein contains a different ¹⁸O/¹⁶O. The EIE is determined from Eq. (1) where terms include R_u and R_t for the ¹⁸O/¹⁶O of the unbound and total O₂ (bound + unbound), respectively, and *f* for the fraction of unbound O₂ in solution.

$$^{18}K = \frac{1 - f}{(R_t/R_u) - f} \quad (1)$$

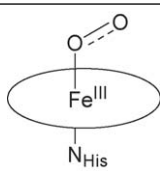
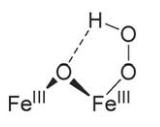
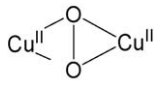
In contrast to EIE measurements, the determination of ¹⁸O KIEs upon reactions which irreversibly consume O₂ requires a sealed reaction vessel. The use of a glass chamber with a movable piston or a collapsible, solvent impervious bag keeps all of the unreacted O₂ dissolved in the solution. The number of moles consumed in the reaction can, therefore, be accurately quantified. At varying stages, samples of unreacted O₂ are collected and the ¹⁸O/¹⁶O determined. The ¹⁸O KIE is derived from Eq. (2), where terms include R₀ for the ¹⁸O/¹⁶O composition at 0% conversion and R_f for the ¹⁸O/¹⁶O ratio at *f* fractional conversion.

$$^{18}k = \left[1 + \frac{\ln(R_f/R_0)}{\ln(1 - f)} \right]^{-1} \quad (2)$$

3. Equilibrium isotope effects on O₂ binding to metalloproteins

Tian and Klinman were the first to measure ¹⁸O EIEs on reversible reactions of O₂ with hemoglobin (Hb), myoglobin (Mb), hemerythrin (Hr) and hemocyanin (Hc) [11]. These proteins bind O₂ with dissociation constants in the micromolar range. The oxygenated species produced have been characterized via a range of spectroscopic methods [4] and the proposed structures are shown in Table 1. In the “end-on” η¹-superoxo structures of oxyHb and oxyMb, the extent of O₂ reduction is less than in oxyHr, which has an η¹-peroxo ligand stabilized by hydrogen bonding, and oxyHc, which has a “side-on” μ-η²:η²-

Table 1
Equilibrium isotope effects (^{18}K) determined for O₂ carrier proteins [11]

Reduced protein	Oxygenated form	^{18}K
Mb Hb		1.0039 ± 0.0002 1.0054 ± 0.0006
Hr		1.0113 ± 0.0005
Hc		1.0184 ± 0.0023

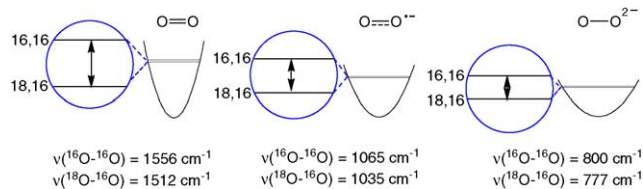


Fig. 2. Changes in O–O force constant and zero point energy level splitting for the light and heavy isotopes upon reduction of O₂.

peroxy ligand bound to two copper ions. The reported ^{18}O EIEs ranging from 1.0039 (Hb) to 1.0184 (Hc) have been attributed to a decrease in total bond order about oxygen [11].

In the absence of a redox metal, addition of electrons to O₂ reduces the bond order at oxygen. As shown in Fig. 2, as the bond order is reduced the O–O force constant also decreases. The attendant decrease in splitting of the isotopic zero point energy levels is believed to be the origin of most heavy atom isotope effects [12]. This simple picture becomes more complicated when bonds formed between oxygen and the redox metal center result in a compensating increase in isotopically sensitive modes. When O₂ binds in an η^1 -manner, there is an isotope effect due to the preferred binding of $^{16}\text{O}-^{16}\text{O}$ over $^{18}\text{O}-^{16}\text{O}$ and a much smaller contribution from the thermodynamic preference for $\text{Fe}-^{16}\text{O}-^{18}\text{O}$ over $\text{Fe}-^{18}\text{O}-^{16}\text{O}$.

In the original studies, simple calculations of ^{18}O EIEs were performed to provide a frame of reference for the bonding changes that occur within the O₂ carrier proteins (Table 2) [10,11]. The assumption was made that the protonated reduced O₂ species (e.g. HO₂[•]) could serve as a model for iron and copper bound O₂. In addition, the preference for H- $^{16}\text{O}-^{18}\text{O}$ over H- $^{18}\text{O}-^{16}\text{O}$ was neglected by averaging the EIEs for the two isotopologues. In the case of complete reduction of O₂ to water, the isotope effect was calculated for two molecules of H₂¹⁶O relative to one molecule of H₂¹⁶O and one molecule of H₂¹⁸O.

The only input data for the calculation of the isotope effects were the stretching frequencies of the reactant and product states, in accord with the formalism developed by Bigeleisen

and Goepfert-Mayer [13]. The EIE is defined according to Eq. (3) as the product of isotopic gas phase partition functions corresponding to zero point energy (ZPE), excited state vibrational energy (EXC) and mass and moments of inertia (MMI) representing translational and rotational degrees of freedom [14]. The partition functions are given by Eqs. (4)–(6), where ν is a normal mode stretching frequency and T is the temperature. In all equations: h is Planck's constant, k is Boltzmann's constant, N is the number of atoms in the reactant ($A \equiv \text{O}_2$) or the metal-bound product (B) and the asterisk designates the site containing ^{18}O . The reduced MMI partition function is expressed as a vibrational product (VP) according to the Redlich–Teller product rule [13,14].

$$\text{EIE} = \text{ZPE} \times \text{EXC} \times \text{MMI} \quad (3)$$

$$\text{ZPE} = \frac{\prod_j^{3N-6} \exp(h\nu_j^{B^*}/2kT) / \exp(h\nu_j^B/2kT)}{\prod_i^{3N-5} \exp(h\nu_i^{A^*}/2kT) / \exp(h\nu_i^A/2kT)} \quad (4)$$

$$\text{EXC} = \frac{\prod_j^{3N-6} (1 - \exp^{-h\nu_j^{B^*}/kT}) / (1 - \exp^{-h\nu_j^B/kT})}{\prod_i^{3N-5} (1 - \exp^{-h\nu_i^{A^*}/kT}) / (1 - \exp^{-h\nu_i^A/kT})} \quad (5)$$

$$\text{MMI} = \text{VP} = \frac{\prod_j^{3N-6} (\nu_j^B/\nu_j^{B^*})}{\prod_i^{3N-5} (\nu_i^A/\nu_i^{A^*})} \quad (6)$$

Calculations of isotope effects on reactions of natural abundance O₂ require the normal mode stretching frequencies for the $^{16}\text{O}-^{16}\text{O}$ and $^{18}\text{O}-^{16}\text{O}$ ($^{16,16}\nu$ and $^{18,16}\nu$). These values were obtained directly from the literature or estimated from known force constants. The results in Table 2 show that, in most cases, ZPE is the dominant contributor to the ^{18}O EIE. In addition, the ZPE accounts for the trend of increasing ^{18}O EIE due to the decrease of the O–O force constant in the reduced oxygen species relative to that in O₂. The contribution from protonation appears to partially offset this effect.

^{18}O EIEs on the reversible formation of the oxygenated molecules in Table 1 have been interpreted in terms of the calculated values in Table 2 [10,11]. It was assumed that the change in the O–O force constant is the major determinant of the isotope effect and, therefore, the ^{18}O EIE should be insensitive to whether the oxygen is bound to a metal or to a proton [11]. Using this simplified model, the ^{18}O EIEs determined for the ferric superoxo species ($\text{Fe}^{\text{III}}-\text{O}_2^{-1}$) in oxyHb (1.0039 ± 0.0002) and oxyMb (1.0054 ± 0.0006) were compared to the calculated value for protonated superoxide (HO₂[•], 1.010). The smaller ^{18}O EIEs in the proteins have been suggested to arise from hydrogen bonding of the terminal oxygen to a distal histidine residue. The

Table 2
Partition functions and ^{18}O EIEs calculated from stretching frequencies [11]

Reaction	ZPE	EXC	MMI	^{18}K
$\text{O}_2 + 2e^- \rightarrow \text{O}_2^{2-}$	1.051	0.998	1.001	1.050
$\text{O}_2 + 1e^- \rightarrow \text{O}_2^-$	1.034	0.999	1.000	1.033
$\text{O}_2 + 1\text{H}^+ + 2e^- \rightarrow \text{HO}_2^-$	1.033	0.997	1.004	1.034
$\text{O}_2 + 1\text{H}^+ + 1e^- \rightarrow \text{HO}_2^\bullet$	1.010	0.999	1.001	1.010
$\text{O}_2 + 2\text{H}^+ + 2e^- \rightarrow \text{HO}_2\text{H}$	1.003	0.998	1.008	1.009
$\text{O}_2 + 4\text{H}^+ + 4e^- \rightarrow 2\text{H}_2\text{O}$	1.041	1.000	0.982	1.023

$\text{Fe}^{\text{III}}\text{-O}_2^{-1}\text{-H}^+$ His interaction would increase the bond order to oxygen and, therefore, decrease the ^{18}O EIE. The physical explanation of the effect is that the stiffening of the potential energy well causes an increase in the zero-point energy level splitting in the product state, making it more like the zero-point energy level splitting in O_2 (cf. Fig. 2).

It has been difficult to evaluate the accuracy of the simplified model in light of the results obtained for the other O_2 -carrier proteins. In the case of oxyHr, the ^{18}O EIE (1.0113 ± 0.0005) is close to the calculated effect for O_2 reduction to H_2O_2 (1.009). This result would appear consistent with the structure where O_2 is reduced by two electrons and a hydrogen bond is formed between $\text{Fe}^{\text{III}}\text{-O}_2^{-11}$ and a hydroxide which bridges the di-iron site. It is more difficult to explain the larger ^{18}O EIE measured for oxyHc (1.0184 ± 0.0023) in the context of the values in Table 2. The binding of O_2 to two copper centers in a $\mu\text{-}\eta^2\text{:}\eta^2$ fashion reduces the ^{18}O EIE relative to that calculated for O_2^{2-} (1.050) but not to the extent observed for H_2O_2 .

4. Equilibrium isotope effects on inorganic peroxide compounds

In an effort to better understand how ^{18}O EIEs reflect bonding within metal– O_2 adducts, we have undertaken studies of inorganic compounds with established vibrational structures. Solomon and coworkers [15] have reported a normal mode analysis of the Hc model compound: $\mu\text{-}\eta^2\text{:}\eta^2\text{-Cu}[\text{HB}(3,5\text{-R}_2\text{pz})_3]_2\text{O}_2$ ($\text{HB}(3,5\text{-R}_2\text{pz})_3$ = tris(pyrazolyl)borate ligand and R = isopropyl or phenyl). This compound was originally reported by Kitajima and co-workers to adopt the same side-on structure as the protein [16]. Using two different assignments of stretching frequencies for the Cu_2O_2 core, we estimate ^{18}O EIEs of 1.017 and 1.021, in excellent agreement with the experimental result for oxyHc. Calculations performed using stretching frequencies from a normal mode analysis of the protein [17] predict an ^{18}O EIE of ~ 1.023 .

While the agreement between the ^{18}O EIE measured for oxyHc and that calculated for $\mu\text{-}\eta^2\text{:}\eta^2\text{-Cu}[\text{HB}(3,5\text{-R}_2\text{pz})_3]_2\text{O}_2$ may be fortuitous, the comparison illustrates a new way to use inorganic compounds for the structural characterization of protein active sites. Before applying the technique further, the ^{18}O EIE for Kitajima's model compound will be experimentally determined and compared to the predicted value. It will be also of interest to compare the results to those obtained for the end-on peroxo compound: *trans*- $\mu\text{-}1,2\text{-}[\text{Cu}(\text{TMPA})_2]_2\text{O}_2$ (TMPA = tris(2-pyridylmethyl)amine) prepared by Karlin and co-workers [18]. Based on the normal mode assignments [19], the ^{18}O EIE is predicted to be ~ 1.023 . Given the small errors in the competitive measurements, it may be possible to experimentally distinguish the ^{18}O EIEs for the end-on and side-on structures.

In an effort to illuminate the more subtle factors which influence ^{18}O EIEs, we have undertaken calculations on the classic η^2 -peroxide compounds: $\text{IrO}_2\text{Cl}(\text{CO})(\text{PPh}_3)_2$, $[\text{IrO}_2(\text{dppe})_2]\text{Cl}$, $[\text{RhO}_2(\text{dppe})_2]\text{Cl}$, $\text{PtO}_2(\text{PPh}_3)_2$, $\text{PdO}_2(\text{PPh}_3)_2$, $\text{NiO}_2(\text{PPh}_3)_2$ and $\text{NiO}_2(\text{CN}^t\text{Bu})_2$ (PPh_3 = triphenylphosphine, dppe = 1,2-

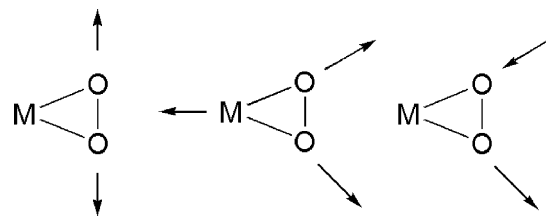


Fig. 3. Isotopically sensitive modes used in the calculation of ^{18}O equilibrium isotope effects on the reversible formation of η^2 -peroxo compounds from O_2 .

bis(diphenylphosphino)ethane, CN^tBu = *tert-n*-butylisocyanide) [20–24]. We have applied Bigeleisen's formalism [14] considering the $\nu_{\text{O-O}}$, the symmetric $\nu_{\text{M-O}}$ and the asymmetric $\nu_{\text{M-O}}$ vibrational modes (Fig. 3). Most of the stretching frequencies used in the calculations were available from previous experimental studies and normal mode analysis [25–28].

Interestingly, the calculations suggest a small contribution from ZPE and a dominant contribution from the MMI in Eq. (3). The physical basis of this result is unclear at the present time. The dominance of the MMI contribution may indicate that the origin of the isotope effect is partially entropic, possibly the loss of isotopically sensitive rotational modes upon binding of O_2 to the heavy metal fragment. The use of gas-phase partition functions to describe translational, rotational and vibrational degrees of freedom for molecules in solution has been previously discussed [12]. In such cases, the isotope effects calculated from Eq. (3) may be accurate although the specific contribution from each partition function cannot be resolved.

^{18}O EIEs on the formation of mononuclear peroxo compounds containing different metals and ligands as well as having different coordination geometries are predicted to fall within a narrow range of 1.026–1.031. This is the result of similar stretching frequencies ($\nu_{\text{O-O}} = 827\text{--}897\text{ cm}^{-1}$, $\nu_{\text{M-O}} = 470\text{--}595\text{ cm}^{-1}$) and shifts upon substituting $^{16}\text{O}\text{-}^{16}\text{O}$ for $^{18}\text{O}\text{-}^{16}\text{O}$ ($\Delta\nu_{\text{O-O}} = 23\text{--}25\text{ cm}^{-1}$, $\Delta\nu_{\text{M-O}} = 9\text{--}10\text{ cm}^{-1}$) [37]. The values are approximately three times greater than the EIE upon reducing O_2 to H_2O_2 (1.009) which has been previously used as a benchmark for identifying metal peroxide intermediates in enzymes.

The calculations on η^2 -peroxo compounds are consistent with the experimental result for oxyHc. Coordination of a second metal center would be expected to decrease the ^{18}O EIE from a value of ca. 1.03. As discussed above, the ^{18}O EIE in the dimer would be reduced relative to a monomer because of the greater splitting of zero-point energy levels associated with the increased number of metal–oxygen bonds. Further studies of ^{18}O EIEs for spectroscopically defined structures are ongoing. In the future, these values can serve as benchmarks for interpreting ^{18}O KIEs on metal-mediated O_2 activation reactions.

5. Kinetic isotope effects on enzymatic activation of O_2

Much progress has been made towards understanding O_2 reactivity of enzymes during the last 10 years. In part, this is due to the development of methods for precisely determining competitive ^{18}O KIEs. It appears that in a number of cases these values can be distinguished from one another and used to infer

Table 3
 ^{18}O kinetic isotope effects (^{18}k) for reactions of O_2 -utilizing enzymes [10]

Enzyme	Proposed reaction	^{18}k
GO		1.0279 ± 0.0006
CAO		1.0101 ± 0.0009
TH		1.0175 ± 0.0019
MMO		1.0152 ± 0.0007
DβM PHM		1.0197 ± 0.0003 1.0173 ± 0.0009

the nature of reactive species. In addition, complex catalytic mechanisms can be simplified since the competitive ^{18}O KIE probes only the steps beginning with the encounter of O_2 up to the first kinetically irreversible step. Table 3 summarizes the reported ^{18}O KIEs as well as the mechanisms which have been proposed for enzymes that activate O_2 prior to the selective oxidation of their substrates [10].

There is an obvious difference in the magnitudes of the ^{18}O KIEs determined for enzymes which reduce O_2 without the formation of new bonds (outer-sphere electron transfer) and those which reduce O_2 by forming metal superoxo and peroxy species (inner-sphere electron transfer). Glucose oxidase (GO), which does not contain a redox metal but a flavin adenine dinucleotide cofactor, falls into the first category [29]. A number of iron and copper enzymes which exhibit oxygenase and oxidase activities appear to fall into the second category [30–34].

Extensive mechanistic studies have demonstrated that GO reacts with O_2 by an outer-sphere electron transfer mechanism [29,35]. ^{18}O KIEs determined for GO containing native and chemically modified flavin cofactors range from 1.0266 ± 0.005 to 1.028 ± 0.004 . These values approach the ^{18}O EIE of 1.033 estimated for the reduction of O_2 to $\text{O}_2^{\bullet-}$. This value has been suggested as an upper limit based on the application of quantum mechanical Marcus theory which takes into consideration the changes in bond length and bond frequency in the transition state [29]. The ^{18}O KIE is surprisingly insensitive to variations in the reaction driving-force as well as to the O_2 reduction rate constants over three orders of magnitude. This behavior has been

explained in terms of a dominant contribution to classical reaction coordinate from reorganization of the protein surroundings. In this model, the isotope effect originates from the quantum mechanical reorganization of the high frequency O–O bond rather than differences in activation barrier height.

Different behavior is expected for inner-sphere electron transfer reactions where the classical reaction coordinate is approximated by a low frequency metal-oxygen stretching mode. For this mechanism, ^{18}O KIEs significantly smaller than those observed for GO have been determined for the iron enzymes: tyrosine hydroxylase (TH, 1.0175 ± 0.0019) and soluble methane monooxygenase (sMMO, 1.0152 ± 0.0007) as well as the copper enzymes: dopamine β -monooxygenase (D β M, 1.0197 ± 0.0003) and peptidylglycine α -hydroxylating monooxygenase (PHM, 1.0173 ± 0.0009) and copper amine oxidase (CAO, 1.0101 ± 0.0009).

^{18}O KIEs on the inner-sphere electron transfer reactions would be expected to exhibit trends similar to those described for the ^{18}O EIEs on reactions of the O_2 carrier proteins (see Section 3). Assuming the ^{18}O EIE is an upper limit, an ^{18}O KIE ≤ 1.005 is expected to characterize the transition state for forming an iron superoxo species. The smallest ^{18}O KIE is seen for CAO which has been attributed to the interaction of the active site copper(II) ion with $\text{O}_2^{\bullet-}$ as it is formed during the reduction of O_2 by the topaquinol cofactor. In contrast to a simple one step electron transfer reaction, the structurally homologous copper monooxygenases, PHM and D β M, have been proposed to reversibly form a copper(II) superoxo species which subsequently abstracts a

Table 4
Partition functions and ^{18}O EIEs calculated from stretching frequencies of inorganic peroxide compounds [25–28] and O_2 [11]

Product ^a	ZPE	EXC	MMI	^{18}K
$\text{IrO}_2\text{Cl}(\text{CO})(\text{PPh}_3)_2$	1.004	0.993	1.031	1.028
$[\text{IrO}_2(\text{dppe})_2]^+$	1.002	0.991	1.036	1.028
$[\text{RhO}_2(\text{dppe})_2]^+$	1.004	0.987	1.040	1.031
$\text{PtO}_2(\text{PPh}_3)_2$	1.002	0.987	1.043	1.031
$\text{PdO}_2(\text{PPh}_3)_2$	1.002	0.988	1.040	1.030
$\text{NiO}_2(\text{CN}^t\text{Bu})_2$	1.000	0.991	1.036	1.026

^a Abbreviations: PPh_3 = triphenylphosphine, dppe = 1,2-bis(diphenylphosphino)ethane, CN^tBu = *tert-n*-butylisocyanide.

hydrogen atom from the substrate C–H bond. In support of this mechanism, an end-on superoxo species has been recently characterized in PHM by X-ray crystallography [36]. Consistent with formation of a copper hydroperoxo species ($\text{Cu}^{\text{II}}-\text{O}_2\text{H}^{-\text{II}}$) in the kinetically irreversible step, the ^{18}O KIEs for PHM and D β M increase to 1.0212 ± 0.0018 and 1.0256 ± 0.0003 when the substrates are deuterium-labeled [33].

6. Kinetic isotope effects on reactions of O_2 with inorganic compounds

Given the ambiguous natures of oxidizing intermediates in enzymes and the complexities associated with the kinetics of catalysis, we have performed studies to evaluate whether benchmark ^{18}O KIEs can be used to characterize specific types of electron transfer reactions. For example, we have reported ^{18}O KIEs on O_2 activation by classic inorganic compounds [37]. The products of these reactions are the η^2 -peroxo compounds: $\text{IrO}_2\text{Cl}(\text{CO})(\text{PPh}_3)_2$, $[\text{IrO}_2(\text{dppe})_2]\text{Cl}$, $\text{PtO}_2(\text{PPh}_3)_2$, $\text{PdO}_2(\text{PPh}_3)_2$, $\text{NiO}_2(\text{PPh}_3)_2$ and $\text{NiO}_2(\text{CN}^t\text{Bu})_2$ for which we have calculated ^{18}O EIEs (Table 4). Measurements of the ^{18}O KIEs and rates were performed using experimental conditions under which O_2 binding was determined to be kinetically irreversible. The results are summarized together with the rate constants for O_2 binding (k_{O_2}) in Table 5.

Table 5
Isotope effects and O_2 binding rate constants for the formation of transition metal peroxide compounds

Product ^a	k_{O_2} ($\text{M}^{-1} \text{s}^{-1}$)	^{18}k	$(^{18}k - 1)/(^{18}K - 1)$
$\text{IrO}_2\text{Cl}(\text{CO})(\text{PPh}_3)_2$	0.17 ± 0.02	1.0268 ± 0.0037^b	0.96
$[\text{IrO}_2(\text{dppe})_2]^+$	2.8 ± 0.4	1.0205 ± 0.0036^b	0.73
$\text{PtO}_2(\text{PPh}_3)_2$	32 ± 7	1.0251 ± 0.0051^c	0.81
$\text{NiO}_2(\text{PPh}_3)_2^d$	3000 ± 80^e	1.0113 ± 0.0027^e	0.40
$\text{NiO}_2(\text{CN}^t\text{Bu})_2$	3300 ± 150^f	1.0069 ± 0.0016^f	0.27
$\text{PdO}_2(\text{PPh}_3)_2$	41100 ± 300	1.0093 ± 0.0029^b	0.31

^a Analysis of products as well as reaction kinetics is described in the original report [37].

^b Measured in DMF and DMSO at $25 \pm 2^\circ\text{C}$.

^c Measured in DMF at $25 \pm 2^\circ\text{C}$.

^d The peroxo compound forms transiently and decomposes to PPh_3 , OPPh_3 , and a Ni^{II} solvento complex.

^e Measured in DMSO at $25 \pm 2^\circ\text{C}$.

^f In the presence of added $[\text{CN}^t\text{Bu}] = 0-0.088 \text{ M}$.

A wide range of normal ^{18}O KIEs from 1.0069 to 1.0268 have been obtained for reactions in which η^2 -peroxo compounds are formed from O_2 . All of the KIEs are less than the calculated ^{18}O EIEs suggesting that the latter values can be viewed as upper limits. As explained above, the ^{18}O KIE is likely to be determined by the weakening of the O–O bond and to a lesser extent the compensating metal–O bond formation. The measured ^{18}O KIEs exhibit a systematic decrease from 1.0268 ± 0.0037 to 1.0069 ± 0.0016 as k_{O_2} increases by approximately five orders of magnitude [37]. These observations suggest that the ^{18}O KIEs reveal variations in the degree of reductive O_2 activation in the transition state.

Reactions where bonds are formed simultaneously with electron transfer are commonly referred to as oxidative additions in organometallic chemistry. Several well-established examples have been reported for H_2 and alkyl halides [38]. However, oxidative addition of O_2 is unique in that the reaction involves converting $^3\text{O}_2$ and a closed shell (singlet) reactant to a product which is a singlet in the ground state. This reaction is formally spin forbidden [39]. Mechanistic pathways, which involve sequential one electron transfer steps, would circumvent the spin conservation problem. One possibility is outer-sphere electron transfer. This type of reaction is characterized by large ^{18}O KIEs of ~ 1.028 , which appear to be relatively independent of reaction rates and thermodynamics (see discussion of glucose oxidase in Section 5). $\text{IrO}_2\text{Cl}(\text{CO})(\text{PPh}_3)_2$ exhibits an ^{18}O KIE in this range, yet an outer-sphere electron transfer mechanism can be ruled out based on the large positive redox potential of the Ir-compound and large negative redox potential of O_2 [37]. An inner-sphere mechanism involving a superoxo intermediate cannot be rigorously excluded for the compounds which exhibit small ^{18}O KIEs. Some of these values are only slightly larger than the ^{18}O EIEs observed for oxyHb and oxyMb. However, the rough trend (Fig. 4) between k_{O_2} and ^{18}k argues against such a changeover in mechanism.

The results are more easily explained within the context of a single type of oxidative addition mechanism where there is a concerted transfer of two electrons upon binding of O_2 in a side-on manner. This observation has important implications for the use

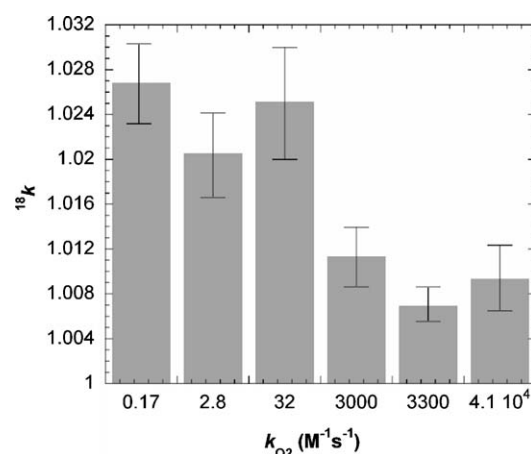


Fig. 4. Correlation of ^{18}O KIEs (^{18}k) to O_2 binding rate constants (k_{O_2}). Data are from Reference [37].

of ^{18}O isotope effects as mechanistic probes, exposing the need for a theoretical framework to explain how a wide range of KIEs can be observed for single class of reactions. We have suggested that the structures of transition states for η^2 -peroxo formation can be characterized by the ratio of kinetic to equilibrium isotope effects: $(^{18}k - 1)/(^{18}K - 1)$ [37]. When this parameter approaches one, the transition state occurs ‘late’ along the reaction coordinate and structurally resembles the peroxide product. Values approaching zero suggest an ‘early’ transition state with a reactant-like (O_2 -like) structure. Consistent with this view, $(^{18}k - 1)/(^{18}K - 1)$ is closest to 1 for $\text{IrCl}(\text{CO})(\text{PPh}_3)_2$ which exhibits the least thermodynamically favorable reaction with O_2 and the lowest k_{O_2} . The $(^{18}k - 1)/(^{18}K - 1)$ decreases systematically to between 0.2 and 0.3 as the reactions become more thermodynamically favorable and the k_{O_2} values increase (Table 5).

The inverse correlation between ^{18}O KIE and k_{O_2} indicates that the barrier to O_2 activation involves extensive reorganization of the O–O bond. Because oxidative addition is a form of electron transfer, Marcus theory is a useful starting point for the quantitative description of how KIEs may vary as a function of driving-force. Eqs. (7) and (8) express the free energy barrier and ^{18}O KIE in terms of an isotope-dependent, inner-sphere reorganization energy (λ_i) and the reaction free energy (ΔG°). Provided the magnitude of λ_i is relatively constant for the series of reactions examined, the equations predict a maximum ^{18}O KIE at $\Delta G^\circ \sim 0$ and a decrease in the KIEs as the reactions become more and less thermodynamically favorable [40].

$$\Delta G_i^\ddagger = \frac{\lambda_i}{4} \left(1 + \frac{\Delta G^\circ}{\lambda_i} \right)^2 \quad (7)$$

$$\Delta G_{18}^\ddagger - \Delta G_{16}^\ddagger = \frac{1}{4}(\lambda_{18} - \lambda_{16}) + \frac{(\Delta G^\circ)^2}{4} \left(\frac{\lambda_{16} - \lambda_{18}}{\lambda_{18}\lambda_{16}} \right) \quad (8)$$

Consistent with this description, O_2 binding to $\text{IrCl}(\text{CO})(\text{PPh}_3)_2$ is close to thermoneutral ($\Delta G^\circ = -5.6 \text{ kcal mol}^{-1}$ in DMF at 25°C) and exhibits an ^{18}O KIE (1.0268) approaching the assumed maximum (1.031). All of the other reactions examined, which are faster and ostensibly more exothermic, exhibit smaller ^{18}O KIEs. A complete analysis of the driving-force dependence of the ^{18}O KIEs will require additional studies of endothermic O_2 binding reactions. The results obtained thus far indicate that thermodynamics is a very important factor to consider when interpreting ^{18}O KIEs on inner-sphere electron transfer reactions, which are the proposed mechanisms in a number of O_2 -activating metalloenzymes.

7. Conclusions

Competitive ^{18}O isotope effects can be used to understand metal-mediated O_2 activation at the level of bonding changes along the reaction coordinate. Normal ^{18}O equilibrium isotope effects characterize the formation of superoxo and peroxo compounds from O_2 . The magnitudes primarily reflect weakening of the O–O bond and, to a lesser extent, compensating metal–oxygen bond formation. Recent results suggest that ^{18}O kinetic isotope effects on reactions which form η^2 -peroxo com-

pounds reveal intimate details about transition state structure. A simplified version of Marcus theory is being tested as a model for the dependence of these isotope effects on the reaction thermodynamics. In this formalism, the contribution of isotope dependent nuclear reorganization to the free energy barrier changes is moderated by the overall reaction driving force. Thus, the thermodynamics associated with inner-sphere electron transfer to O_2 is important to consider when interpreting ^{18}O KIEs on reactions of metalloenzymes and inorganic compounds. Based on these early studies, we are optimistic about future applications of ^{18}O isotope effects as mechanistic probes of O_2 activation in chemical and biological catalysis.

8. General experimental

The compounds described in this paper were prepared following published procedures [41–45]. Their purities were confirmed by elemental analysis, multinuclear NMR and comparison with published molar extinction coefficients. ‘‘Anhydrous’’ brand DMF and DMSO solvents from Burdick and Jackson were used as received. All isotope effects and rate constants are reported at $25 \pm 2^\circ\text{C}$ with $\pm 2\sigma$ errors. Kinetic data were obtained using an Agilent 8453 UV–vis spectrophotometer or an OLIS RSM1000 stopped-flow spectrophotometer. Isotope ratio analysis of CO_2 samples was performed using a Micromass Isoprime stable isotope mass spectrometer equipped with dual-inlet system (Johns Hopkins University, Department of Earth and Planetary Sciences).

Acknowledgments

We gratefully acknowledge grants from the U.S. National Science Foundation (CAREER CHE0449900 to J.P.R.) and the U.S. National Institutes of Health (RO1 GM28962 to K.D.K.) for support of this work.

References

- [1] B. Meunier (Ed.), *Biomimetic Oxidations Catalyzed by Transition Metal Complexes*, Imperial College Press, London, 2000.
- [2] P.R. Ortiz de Montellano (Ed.), *Cytochrome P-450: Structure Mechanism and Biochemistry*, second ed., Plenum Press, New York, 1995.
- [3] M. Costas, M.P. Mehn, M.P. Jensen, L. Que Jr., *Chem. Rev.* 104 (2004) 939.
- [4] J.S. Valentine, C.S. Foote, A. Greenberg, J.F. Liebman (Eds.), *Active Oxygen in Biochemistry*, Chapman and Hall, Glasgow, 1995, pp. 44–47, 213–222.
- [5] M. Sommerhalter, R.L. Lieberman, A.C. Rosenzweig, *Inorg. Chem.* 44 (2005) 770.
- [6] E.I. Solomon, T.C. Brunold, M.I. Davis, J.N. Kemsley, S.-K. Lee, N. Lehnert, F. Neese, A.J. Skulan, Y.-S. Yang, J. Zhou, *Chem. Rev.* 100 (2000) 235.
- [7] E.C. Niederhoffer, J.H. Timmons, A.E. Martell, *Chem. Rev.* 84 (1984) 137.
- [8] C.J. Cramer, W.B. Tolman, K.H. Theopold, A.L. Rheingold, *Proc. Natl. Acad. Sci. U.S.A.* 100 (2003) 3635.
- [9] R.D. Guy, M.F. Fogel, J.A. Berry, T.C. Hoering, *Prog. Photosynth. Res.* 3 (1987) 597.
- [10] J.P. Roth, J.P. Klinman, in: A. Kohen, H.H. Limbach (Eds.), *Isotope Effects in Chemistry and Biology*, CRC Press, Boca Raton, 2005.

- [11] G. Tian, J.P. Klinman, *J. Am. Chem. Soc.* 115 (1993) 8891, references therein.
- [12] M. Wolfsberg, *Acc. Chem. Res.* 5 (1972) 225.
- [13] J. Bigeleisen, M. Goepfert-Mayer, *J. Chem. Phys.* 15 (1947) 261.
- [14] P.W. Huskey, in: P.F. Cook (Ed.), *Enzyme Mechanism from Isotope Effects*, CRC Press, Boca Raton, 1991, pp. 37–72.
- [15] M.J. Baldwin, D.E. Root, J.E. Pate, K. Fujisawa, N. Kitajima, E.I. Solomon, *J. Am. Chem. Soc.* 114 (1992) 10421.
- [16] N. Kitajima, K. Fujisawa, Y. Moro-oka, K. Toriumi, *J. Am. Chem. Soc.* 111 (1989) 8975.
- [17] J. Ling, L.P. Nestor, R.S. Czernuszewicz, T.G. Spiro, R. Fraczkiewicz, K.D. Sharma, T.M. Loehr, J. Sanders-Loehr, *J. Am. Chem. Soc.* 116 (1994) 7682.
- [18] R.R. Jacobson, Z. Tyeklar, A. Farooq, K.D. Karlin, S. Liu, J. Zubieta, *J. Am. Chem. Soc.* 110 (1988) 3690.
- [19] M.J. Baldwin, P.K. Ross, J.E. Pate, Z. Tyeklár, K.D. Karlin, E.I. Solomon, *J. Am. Chem. Soc.* 113 (1991) 8671.
- [20] L. Vaska, L.S. Chen, C.V. Senoff, *Science* 174 (1971) 587.
- [21] J.A. McGinnety, J.A. Ibers, *J. Chem. Soc., Chem. Commun.* (1968) 235.
- [22] J.P. Birk, J. Halpern, A.L. Pickard, *J. Am. Chem. Soc.* 90 (1968) 4491.
- [23] G. Wilke, H. Schott, P. Heimbach, *Angew. Chem., Int. Ed. Engl.* 6 (1967) 92.
- [24] S. Otsuka, T. Yoshida, Y. Tatsuno, *J. Am. Chem. Soc.* 93 (1971) 6462.
- [25] R.W. Horn, E. Weissberger, J.P. Collman, *Inorg. Chem.* 9 (1970) 2367.
- [26] C. Pettinari, F. Marchetti, A. Cingolani, G. Bianchini, A. Drozdov, V. Vertlib, S. Troyanov, *J. Organomet. Chem.* 651 (2002) 5.
- [27] A. Nakamura, Y. Tatsuno, M. Yamamoto, S. Otsuka, *J. Am. Chem. Soc.* 93 (1971) 6052.
- [28] P.J. Hayward, D.M. Blake, G. Wilkinson, C.J. Nyman, *J. Am. Chem. Soc.* 92 (1970) 5873.
- [29] J.P. Roth, R. Wincek, G. Nodet, D.E. Edmondson, W.S. McIntire, J.P. Klinman, *J. Am. Chem. Soc.* 126 (2004) 15120.
- [30] W.A. Francisco, G. Tian, P.F. Fitzpatrick, J.P. Klinman, *J. Am. Chem. Soc.* 120 (1998) 4057.
- [31] S.S. Stahl, W.A. Francisco, M. Merx, J.P. Klinman, S.J. Lippard, *J. Biol. Chem.* 276 (2001) 4549.
- [32] G. Tian, J.A. Berry, J.P. Klinman, *Biochemistry* 33 (1994) 226.
- [33] W.A. Francisco, N.J. Blackburn, J.P. Klinman, *Biochemistry* 42 (2003) 1813.
- [34] S.A. Mills, Y. Goto, Q. Su, J. Plastino, J.P. Klinman, *Biochemistry* 41 (2002) 10577.
- [35] J.P. Roth, J.P. Klinman, *Proc. Natl. Acad. Sci. U.S.A.* 100 (2003) 62.
- [36] S.T. Prigge, B.A. Eipper, R.E. Mains, L.M. Amzel, *Science* 304 (2004) 864.
- [37] M.P. Lanci, D.W. Brinkley, K.L. Stone, V.V. Smirnov, J.P. Roth, *Angew. Chem., Int. Ed. Engl.* 44 (2005) 7273.
- [38] R.H. Crabtree, *Organometallic Chemistry of the Transition Metals*, Wiley, New York, 2001.
- [39] C.R. Landis, C.M. Morales, S.S. Stahl, *J. Am. Chem. Soc.* 126 (2004) 16302.
- [40] A similar model has been applied to proton transfer reaction: see. A similar model has been applied to proton transfer reaction: see M.M. Kreevoy, R. Eliason, R.A. Landholm, T.S. Straub, J.L. Melquist, *J. Phys. Chem.* 76 (1972) 2951.
- [41] J.P. Collman, C.T. Sears Jr., M. Kubota, *Inorg. Synth.* 28 (1990) 92.
- [42] L. Vaska, D.L. Catone, *J. Am. Chem. Soc.* 88 (1966) 5324.
- [43] R. Ugo, F. Cariati, G. La Monica, *Inorg. Synth.* 11 (1968) 105.
- [44] S.D. Ittel, *Inorg. Synth.* 28 (1990) 98.
- [45] S. Otsuka, A. Nakamura, Y. Tatsuno, *J. Am. Chem. Soc.* 91 (1969) 6994.